GEOLOGICA CARPATHICA, AUGUST 2019, 70, 4, 355–369 doi: 10.2478/geoca-2019-0020

The calcareous nannofossils and magnetostratigraphic results from the Upper Tithonian–Berriasian of Feodosiya region (Eastern Crimea)

VLADIMIR ARKADIEV[1,✉], MARINA LESCANO[2], ANDREA CONCHEYRO[2], ANDREY GUZHIKOV[3] and EVGENY BARABOSHKIN[4]

[1]Saint Petersburg State University, University Embankment 7/9, 199034 Saint Petersburg, Russia; ✉arkadievvv@mail.ru
[2]Instituto de Estudios Andinos Don Pablo Groeber, Conicet-Universidad de Buenos Aires, 1428, Buenos Aires, Argentina; andrea@gl.fcen.uba.ar
[3]Saratov State University, Astrahanskaya Street 83, 410012 Saratov, Russia; aguzhikov@yandex.ru
[4]Moscow State University, Leninskie Gory Street 1,119991 Moscow, Russia; ejbaraboshkin@mail.ru

(Manuscript received March 27, 2019; accepted in revised form June 17, 2019)

Abstract: This article is concerned with nannofossil study of Tithonian–Berriasian sediments of Eastern Crimea. The NJT16, NJT17a, NJT17b, NKT, and NK1 nannofossil zones were determined. The occurrence of *Nannoconus kamptneri minor*, one of the potential marker-types of the Tithonian–Berriasian boundary (the base of the NKT Zone) of the Tethyan sequence in the Feodosiyan section is assigned here to the *Pseudosubplanites grandis* ammonite Subzone and the magnetic Chron M18n. The base of the NKT Zone is closer to the *Grandis* Subzone base than to the base of the *Jacobi* Subzone. Contradictions in the interpretation of magnetic chrons obtained by the present authors (Arkadiev et al. 2018) and by Bakhmutov et al. (2018) might be caused by mistakes admitted in the latter work on the compiled section.

Keywords: calcareous nannofossils, magnetostratigraphy, Tithonian, Berriasian, Eastern Crimea.

Introduction

The section of the Tithonian–Berriasian boundary sediments located in the Feodosiya area, Eastern Crimea, has been attracting the attention of researchers for over 100 years. The study of the Feodosiyan section began in the XIX century (Sokolov 1886; Retowski 1893) and has been reviewed in a monograph (Arkadiev et al. 2012). Guzhikov et al. (2012) first provided a description of the compiled Upper Tithonian–Lower Berriasian section situated at the southern edge of the town of Feodosiya within the area of Dvuyakornaya Bay Saint Ilya Cape, and Feodosiisky Cape. Later, Arkadiev et al. (2018) and Baraboshkin et al. (2016a) detailed the structure of the section, summarized and analysed data on bio- and magnetostratigraphic stratification of the section, and provided zonal schemes on ammonites, calpionellids, foraminifera, ostracods, dinocysts, and trace fossils. The section covers an interval from the Upper Tithonian (*Microcanthum* and *Andreaei* ammonite Zones) to the Lower Berriasian (*Jacobi* Zone), where corresponding of the magnetic chrons from M20n to M17r inclusively were determined. The thickness of the sediments between the uppermost findings of Upper Tithonian ammonites and lowest findings of Berriasian ammonites is at least 100 metres. Therefore, the boundary between the Jurassic and Cretaceous was assumed by the authors to be the base of the *Berriasella jacobi* ammonite Zone but it has not been accurately positioned in the section. Higher levels of the Berriasian section (*Occitanica* and *Boissieri* Zones) were studied within the Zavodskaya Balka quarry in the Feodosiya area (Arkadiev et al. 2015, 2017, 2018; Savelieva et al. 2017; Baraboshkin et al. 2017, 2019). There, on the basis of bio- and magnetostratigraphic data the boundary between the Berriasian and Valanginian was first justified.

Previously, the authors of this paper have not studied calcareous nannofossils in the Feodosiyan section.

To recent times, the data on the distribution of calcareous nannofossils in the Tithonian–Berriasian of Mountain Crimea has been quite poor. Matveyev, in his studies of the Tithonian–Berriasian in Eastern Crimea (Matveyev 2009, 2010), including the sections of the Thonas River and Feodosiya, mentioned a pretty poor collection of nannofossils from those sites. He assigned the Tithonian/Berriasian boundary to the first appearance datums (FADs) of *Nannoconus steinmannii steinmannii, N. steinmannii minor* and *N. dolomiticus,* although the former subspecies was found in the Tithonian as well (Matveyev 2009). According to the widely accepted concepts, *Nannoconus steinmannii* Kamptner is a species determining the Jurassic–Cretaceous boundary (see Casellato 2010; Wimbledon et al. 2011). Stoykova et al. (2018a,b), however, provided calibrated ammonite and calcareous nannofossil documentation from Bulgaria, showing that *Nannoconus steinmannii minor* appeared above the bases of the *Berriasella jacobi* Zone and *Calpionella alpina* Subzone, and *Nannoconus steinmannii steinmannii* appeared even very up-section; the latter bioevent correlates with the *Calpionella elliptica* Subzone and the M17r magnetic Chron. Actually, the calcareous

nannofossil event which is closer to the base of the *Calpionella alpina* Subzone, namely to the base of the Berriasian, is *Nannoconus wintereri* first occurrence. This bioevent shows relatively short vertical dispersal in many sections, such as the Bosso Valley, Font de St Bertrand, Lókút, Nutzhof, Puerto Escaño (Casellato 2010; Grabowski et al. 2017; Svobodová & Košťák 2016; Stoykova et al. 2018a,b).

Based on this data and taking into consideration the information on the distribution of foraminifera and palynomorphs within the section of the Thonas River, Dorotyak et al. (2009) determined the boundary between Tithonian and Berriasian from the occurrence of the assemblage of foraminifera *Protopeneroplis ultragranulatus–Siphoninella antique*, calcareous nannofossil assemblage of *Crepidolithus crassus* (Deflandre), *Nannoconus dolomiticus* Cita, as well as *Nannoconus steinmannii* Kamptner and *Lithraphidites carniolensis*, and the dinocyst species *Pseudoceratium pelliferum* (Pp.). In the boundary interval of the Thonas River section, there is a suggestion to distinguish a *Zeugrhabdotus embergeri* Zone in the Upper Tithonian and a *Lithraphidites carniolensis* Zone in the Lower Berriasian at the base of which a "bloom" of nannoconids was observed (Dorotyak et al. 2009). Unfortunately, calcareous nannofossils were not figured in that article.

Recently, a team of European researches published independent bio- and magnetostratigraphic data and interpretation that they obtained in studying the *Jacobi* Zone of the Feodosiyan section (Bakhmutov et al. 2018), which significantly differs from our outcomes made earlier (Arkadiev et al. 2018; Guzhikov et al. 2012;). Discussion of these contradictions along with presentation of new data on calcareous nannofossils is the purpose of this article.

Geological setting

The compiled Feodosiyan section comprises several independent sections (outcrops 2901, 2922-2924, 3112, 3113, 2456, 2927, 2920, and 2921) of the Dvuyakornaya Formation exposed as coastal cliffs at the Black Sea beach in the Feodosiisky Cape, Saint Ilya Cape, and in Dvuyakornaya Bay, at the southern edge of the Feodosiya town (Fig. 1) (see Guzhikov et al. 2012; Arkadiev et al. 2018). The section represents calciturbidites, debrites and pelagic deposits from the deeper part of a distally steepened ramp (Guzhikov et al. 2012; Baraboshkin et al. 2016b) of about 400 m total thickness. The bed dips vary from north-east to north-west with dip angles basically varying from 20° to 40°.

Compilation of such a complex section covering the Upper Tithonian–Lower Berriasian (*Jacobi* Zone) interval was a challenging task considering the numerous disjunctive dislocations, gaps in exposure and absence of lithological markers which might be traced from outcrop to outcrop. The base of the package of Feodosiyan Marls, with more or less lateral continuity, looks like a lucky exception. Guzhikov et al. (2012) assumed that the upper beds in sections of the Dvuyakornaya Bay (outcrop 2924) and Feodosiisky Cape (outcrop 2921) were an analogue of the thick (1.5–3.0 m) conglomerate-type limestone channel turbidite at the base of the Cape Saint Ilya section (outcrop 2456). Inconsistency of such assumptions becomes clearly understandable when one observes the sections at a distance from the sea. The results of revision of the section we made in 2016 indicated that beds of conglomerate-type limestones in outcrops 2924 and 2921 that looked like a three-metre bed of similar limestone in the Cape Saint Ilya

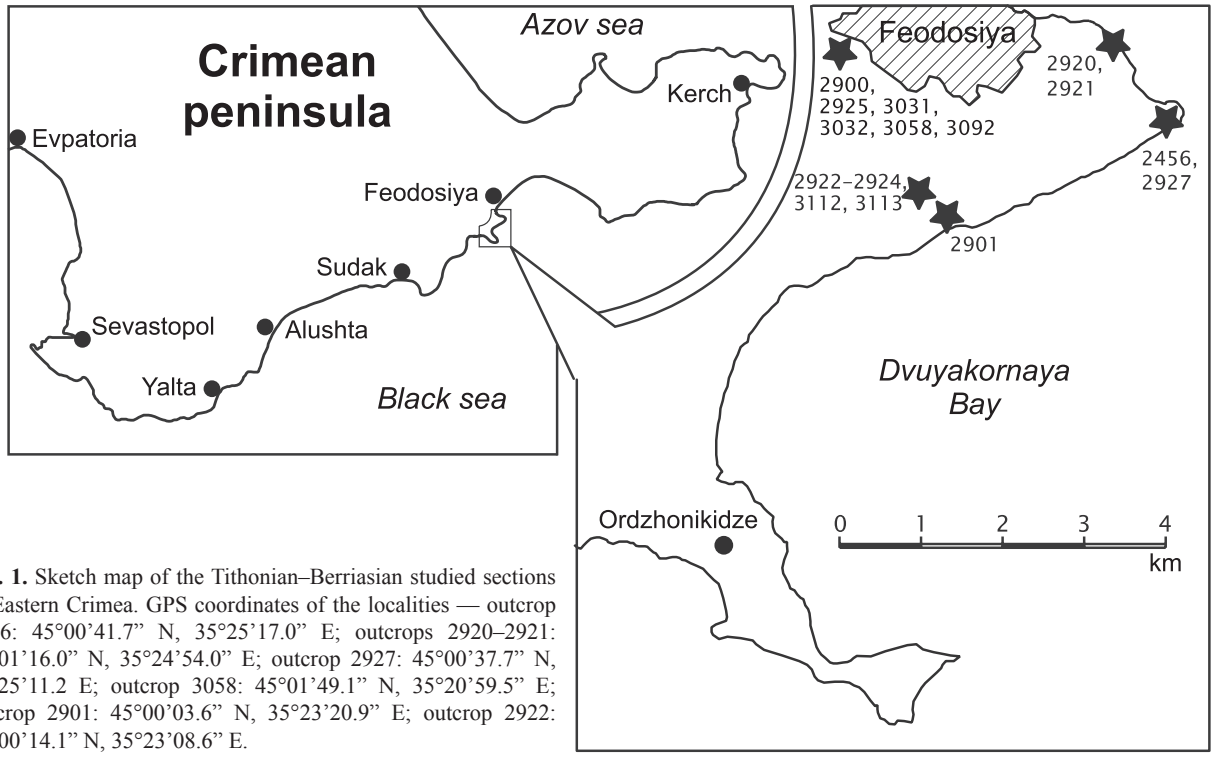

Fig. 1. Sketch map of the Tithonian–Berriasian studied sections in Eastern Crimea. GPS coordinates of the localities — outcrop 2456: 45°00'41.7" N, 35°25'17.0" E; outcrops 2920–2921: 45°01'16.0" N, 35°24'54.0" E; outcrop 2927: 45°00'37.7" N, 35°25'11.2 E; outcrop 3058: 45°01'49.1" N, 35°20'59.5" E; outcrop 2901: 45°00'03.6" N, 35°23'20.9" E; outcrop 2922: 45°00'14.1" N, 35°23'08.6" E.

section should actually be regarded as older and younger beds, respectively (Arkadiev et al. 2018). These limestones are channel turbidites in origin and, therefore, their thickness is not consistent. At the present time, it became evident that the Feodosiyan Upper Tithonian–Lower Berriasian compiled section includes three stratigraphic gaps of undetermined thicknesses (Fig. 2). Some indirect data (including magnetic susceptibility) allow us to assume that these gaps hardly exceed the first tens of metres.

The Zavodskaya Balka quarry on the outskirts of Feodosiya Town has provided outcrops of the well-developed Sultanovskaya Formation, basically represented by grey pelagic mudstones (Baraboshkin et al. 2019) of about 100 m thickness with Berriasian ammonites of the *Occitanica* and *Boissieri* Zones (outcrops 2900, 2925, 3031, 3032, 3058, and 3092). Calcareous nannofossils from this part of the section have been studied for the first time ever.

Material and methods

Samples to conduct bio- and magnetostratigraphic studies on the "sample to sample" system were taken in the process of field research. A total of 43 samples from the four Crimean sections were examined for calcareous nannofossils, 38 of them being fossiliferous.

Smear slides were prepared following the smear slide technique (Edwards 1963) and the slides were fixed with UV curing Norland Optical Adhesive. Systematic determinations and photographs were established by a standard LEICA DMLP petrographic microscope with 1000× magnification under polarized light. The fossiliferous samples are housed in the Department of Geological Sciences, University of Buenos Aires, under the acronym BACF-NP 4147-4189.

Calcareous nannofossil bioevents and zonation

The recorded assemblages of calcareous nannofossils from Eastern Crimea are diverse enough and are represented by 67 Tethyan species. The full list of the nannofossils recovered is provided in Table 1. Estimation of the nannofossil total abundance has been recorded as follow (Table 2): VA (very abundant): ≥15 specimens per field of view; A (abundant): 5–15 specimens per field of view; C (common): 1–5 specimens per field of view; F (few): 1 specimen every 1–10 fields of view; R (rare): 1 specimen every 11–100 fields of view.

The nannofossil species from the Crimean sections are illustrated in Figs. 3–5. The Crimean nannofossils assemblages show low abundance, moderate state of preservation and are mainly dominated by abundant *Watznaueria fossacincta* (Fig. 4G), *W. britannica* (Fig. 4C), *W. barnesiae* (Fig. 4E), and *Cyclagelosphaera* sp.

A specific horizon contains some Early Jurassic species such as *Parhabdolithus robustus* (Fig. 5A,B) and *Crepidolithus* sp. (Fig. 5C,D), which were reworked from older strata.

Bralower et al. (1989) proposed a calcareous nannofossil zonation for the Jurassic and Cretaceous based on southern European land sections and sites from the western North Atlantic Ocean (Fig. 6). In particular, the NJK Zone straddled the Tithonian–Berriasian boundary. The NJK Zone is divided into four subzones (NJK-A, NJK-D, NJK-C, and NJK-D), their lower boundaries being marked at the FADs of *Helenea chiastia, Umbria granulosa granulosa, Rotelapillus laffittei*, and *Nannoconus steinmannii,* respectively. These authors placed the base of the Berriasian in the middle of the NJK-C Subzone, which coincides with the base of M18 magnetic Chron, the base of the *Berriasella jacobi* ammonoid Zone, and the base of the *Calpionella alpina* Subzone. Besides, Bralower et al. (1989) correlated their zones with other bioevents such as the FADs of *Rhagodiscus asper* and *Nannoconus wintereri.*

More recently, Casellato (2010) proposed a new calcareous nannofossil biostratigraphic scheme for the Tithonian–Early Berriasian established for the Southern Alps in Northern Italy. She defined the NJT 16, NJT 17, and NKT Zones on the basis of FADs of *Helenea chiastia, Nannoconus globulus minor,* and *Nannoconus steinmannii minor*, respectively, and placed the base of the Berriasian at the base of NKT Zone (the FAD of *N. steinmannii minor*). In the Crimean sections, five markers of calcareous nannofossils were determined like in other Tethyan sections (see Bralower et al. 1989; Casellato 2010). These bioevents have defined the studied interval as Early Tithonian to Berriasian in age. In particular, the NJT 16-17, NKT, and NK-1 Tethyan Zones have been determined (Fig. 2).

The FO of *Helenea chiastia* (sample 2901-19, Fig. 4S) has been assumed as the first recorded event (Bralower at el. 1989; Casellato 2010); it defines the base of NJT 16a, which is correlated with the top of the Lower Tithonian. No ammonites typical for Early Tithonian were detected in this part of the section.

Up-section, the FO of *Hexalithus strictus* (sample 3112-3, Fig. 3F) has been used to determine the NJT 17a Subzone (middle part). In the Feodosiyan section, it correlates directly with the ammonite *Berriasella chomeracensis*, the latter being characteristic for the Lower Berriasian. Findings of the Upper Tithonian ammonites *Paraulacosphinctes transitorius*, *P.* cf. *senoides* were recorded approximately 110 m down-section. It is likely that the base of the NJT 17a Subzone is located down the section, within the Upper Tithonian, as well as in the Kopanista section (Stoykova et al. 2018a).

The FO of *Nannoconus wintereri* (sample 2456-31, Fig. 5O,P), is a bioevent that determines the base of the NJT 17b Subzone (Casellato 2010). *N. wintereri* was detected in the section definitely higher than the Lower Berriasian finds of *Pseudosubplanites* cf. *lorioli* and *Delphinella* cf. *obtusenodosa*.

The FO of *Nannoconus kamptneri minor* (sample 2456-51) (Fig. 5Q,R) defines the base of the NKT Zone which is assigned to the Berriasian. A number of researches considered this event to be a reliable marker of the Tithonian–Berriasian boundary (Michalík & Reháková 2011; Wimbledon et al.

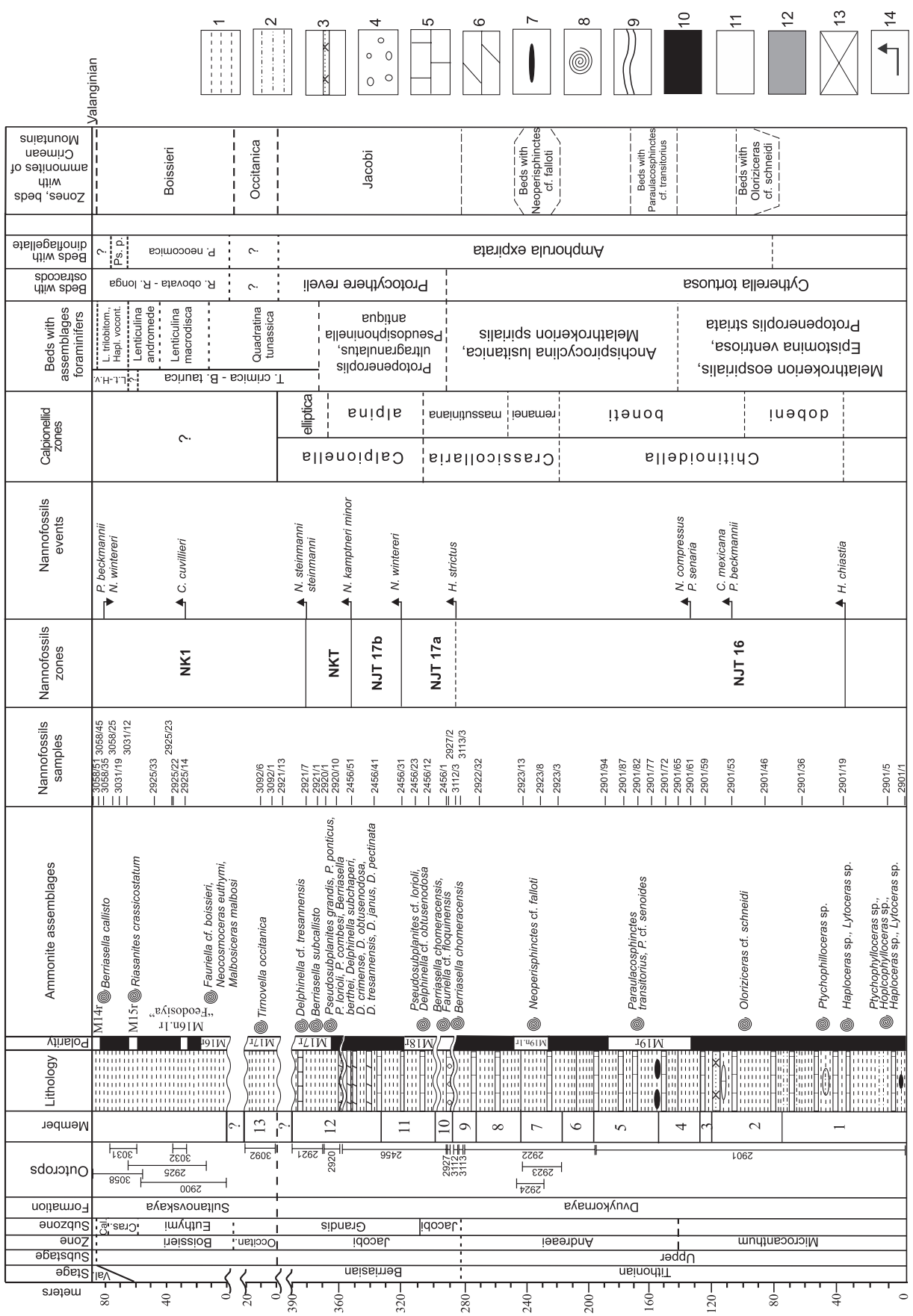

Fig. 2. Compiled Tithonian–Berriasian section of Eastern Crimea and its bio-stratigraphic and magnetostratigraphic zonation. Legend: 1 — clay, 2 — aleurolite, 3 — calcareous sandstone, 4 — conglomerate, 5 — limestone, 6 — marlstone, 7 — siderite lenses, 8 — ammonites, 9 — not observed, 10–12 — geomagnetic polarity: 10 — normal, 11 — reverse, 12 — anomalous. 13 — missing data, 14 — FADs.

Table 1: List of recorded calcareous nannofossil species of Eastern Crimea.

		Section			
		1	2	3	4
1	*Axopodorhabdus cylindratus* (Noël, 1965) Wind and Wise in Wise and Wind, 1977				X
2	*Biscutum* sp.				X
3	*Bukrylithus ambiguus* Black, 1971				X
4	*Conusphaera mexicana* Trejo, 1969	X	X	X	X
5	*Cretarhabdus madingleyensis* (Black, 1971) Crux, 1989	X	X		
6	*Crepidolithus* sp.			X	X
7	*Cruciellipsis cuvillieri* (Manivit, 1966) Thierstein, 1971				X
8	*Cyclagelosphaera argoensis* Bown, 1992	X			
9	*Cyclagelosphaera brezae* Applegate & Bergen, 1988	X	X		X
10	*Cyclagelosphaera deflandrei* (Manivit, 1966) Roth, 1973	X			X
11	*Cyclagelosphaera lacuna* Varol & Girgis 1994	X		X	X
12	*Cyclagelosphaera margerelii* Noël, 1965	X	X	X	X
13	*Diazomatolithus galicianus* de Kaenel & Bergen, 1996				X
14	*Diazomatolithus lehmanii* Noël, 1965	X	X	X	X
15	*Eiffellithus primus* Applegate & Bergen, 1988				X
16	*Ethmorhabdus gallicus* Noël, 1965	X	X		X
17	*Ethmorhabdus hauterivianus* (Black, 1971) Applegate et al. in Covington & Wise, 1987				X
18	*Hayesites irregularis* (Thierstein in Roth & Thierstein, 1972) Applegate et al. in Covington & Wise, 1987				X
19	*Helenea chiastia* Worsley, 1971	X			X
20	*Helenea quadrata* (Worsley, 1971) Rutledge & Bown in Bown et al., 1998		X		X
21	*Helenea staurolithina* Worsley, 1971	X	X	X	X
22	*Hexalithus noeliae* Loeblich & Tappan, 1966	X			
23	*Hexalithus strictus* Bergen, 1994	X			X
24	*Lithraphidites carniolensis* Deflandre, 1963				X
25	*Manivitella pemmatoidea* (Deflandre in Manivit, 1965) Thierstein, 1971	X			X
26	*Micrantholithus hoschulzii* (Reinhardt, 1966) Thierstein, 1971				X
27	*Micrantholithus obtusus* Stradner, 1963				X
28	*Micrantholithus parvistellatus* Varol 1991				X
29	*Micrantholithus* sp.				X
30	*Nannoconus compressus* Bralower & Thierstein in Bralower et al., 1989	X			X
31	*Nannoconus globulus* subsp. *globulus* Brönnimann, 1955				X
32	*Nannoconus globulus* subsp. *minor* (Brönnimann, 1955) Bralower in Bralower et al., 1989		X	X	X
33	*Nannoconus kamptneri* subsp. *kamptneri* Brönnimann, 1955				X
34	*Nannoconus kamptneri* subsp. *minor* (Brönnimann, 1955) Bralower in Bralower et al., 1989		X	X	X
35	*Nannoconus* sp.		X	X	X
36	*Nannoconus steinmannii* subsp. *minor* (Kamptner, 1931) Deres and Achéritéguy, 1980			X	X
37	*Nannoconus steinmannii* subsp. *steinmannii* Kamptner, 1932			X	X
38	*Nannoconus wintereri* Bralower & Thierstein, in Bralower et al. 1989		X	X	X
39	*Parhabdolithus robustus* Noël, 1965	X	X		
40	*Percivalia fenestrata* (Worsley, 1971) Wise, 1983				X
41	*Polycostella beckmannii* Thierstein, 1971	X			X
42	*Polycostella senaria* Thierstein, 1971	X			X
43	*Polycostella* sp.				X
44	*Retecapsa angustiforata* Black, 1971				X
45	*Retecapsa crenulata* (Bramlette & Martini, 1964) Grün in Grün and Allemann, 1975				X
46	*Retecapsa octofenestrata* (Bralower in Bralower et al., 1989) Bown in Bown & Cooper, 1998				X
47	*Retecapsa schizobrachiata* (Gartner, 1968) Grün in Grün and Allemann, 1975				X
48	*Retecapsa surirella* (Deflandre & Fert, 1954) Grün in Grün and Allemann, 1975				X
49	*Rhagodiscus adinfinitus* Bown, 2005				X
50	*Rhagodiscus asper* (Stradner, 1963) Reinhardt, 1967				X
51	*Speetonia colligata* Black, 1971				X
52	*Staurolithites* sp.				X
53	*Tubodiscus verenae* Thierstein, 1973				X
54	*Umbria granulosa* Bralower & Thierstein in Bralower et al., 1989				X
55	*Watznaueria barnesiae* (Black in Black & Barnes, 1959) Perch-Nielsen, 1968	X	X	X	X
56	*Watznaueria biporta* Bukry, 1969				X
57	*Watznaueria britannica* (Stradner, 1963) Reinhardt, 1964	X	X	X	X
58	*Watznaueria communis* Reinhardt, 1964	X	X	X	X
59	*Watznaueria fossacincta* (Black, 1971) Bown in Bown & Cooper, 1989	X	X		X
60	*Watznaueria manivitiae* Bukry, 1973	X	X	X	X
61	*Watznaueria ovata* Bukry, 1969		X		
62	*Zeugrhabdotus diplogrammus* (Deflandre in Deflandre & Fert, 1954) Burnett in Gale et al., 1996				X
63	*Zeugrhabdotus embergeri* (Noël, 1959) Perch-Nielsen, 1984	X	X	X	X
64	*Zeugrhabdotus erectus* (Deflandre in Deflandre & Fert, 1954) Reinhardt, 1965	X	X		X
65	*Zeugrhabdotus fissus* Grün & Zweili, 1980		X		
66	*Zeugrhabdotus* sp.			X	X
67	*Tegumentum* sp.				X

Table 2: Semi-quantitative estimation of nannofossil' abundance in the studied samples.

Section 4	*Ethmorhabdus gallicus*	*Nannoconus sp.*	*Watznaueria manivitiae*	*Staurolithites sp.*	*Micrantholithus hoschulzii*	*Conusphaera mexicana*	*Cyclagelosphaera brezae*	*Cyclagelosphaera margerelii*	*Watznaueria barnesiae*	*Diazomatolithus lehmanii*	*Rhagodiscus asper*	*Nannoconus kamptneri subsp. minor*	*Nannoconus kamptneri subsp. kamptneri*	*Nannoconus globulus subsp. minor*	*Watznaueria britannica*	*Hexalithus strictus*	*Polycostella senaria*	*Nannoconus steinmannii subsp. steinmannii*	*Zeugrhabdotus embergeri*	*Helenea chiastia*	*Watznaueria communis*	*Percivalia fenestrata*	*Retecapsa angustiforata*	*Micrantholithus sp.*	*Micrantholithus parvistellatus*	*Zeugrhabdotus sp.*	*Biscutum sp.*	*Crepidolithus sp.*	*Nannoconus wintereri*	*Eiffellithus primus*	*Cruciellipsis cuvillieri*
3058-51			R	R		R	C	C	A	C	C							R	F	C			R								C
3058-45			R					A	A	R	F		R						R	R			R								R
3058-35								C	C	F									F											R	
3058-25			F	R	F	F		E	C			R		F	R				F	R									R	R	R
3031-19								C	C	C	C	R		F					F	R			R								R
3031-12		C	C		C			C	A	R	C	C	R		R			C	R	R	R		R	C			R		R		
2925-33		R		R		C	C	C	A	F	F	F		C				C	F	C										R	F
2925-23-22						R		A	A	R				R	C			C			C								R		
2925-14		C	C			R		C	A	C	R		R	C	C				R	R	C		R	C	F	R	R	R	R	R	R
3092-6					F	F	C	C	A	F	F	F	C	E	C	F	C	F	F	F	F	R									
3092-1	F	C	C	F	C	R	F	A	C	F	F	F	R	F	F	R															

Section 4	*Lithraphidites carniolensis*	*Nannoconus globulus subsp. globulus*	*Nannoconus steinmannii subsp. minor*	*Cyclagelosphaera deflandrei*	*Polycostella sp.*	*Micrantholithus obtusus*	*Polycostella beckmannii*	*Watznaueria fossacincta*	*Umbria granulosa*	*Retecapsa surirella*	*Watznaueria biporta*	*Zeugrhabdotus diplogrammus*	*Rhagodiscus adinfinitus*	*Helenea staurolithina*	*Zeugrhabdotus erectus*	*Speetonia colligata*	*Diazomatolithus galicianus*	*Ethmorhabdus hauterivianus*	*Tubodiscus verenae*	*Cocosfera*	*Helenea quadrata*	*Retecapsa crenulata*	*Hayesites irregularis*	*Cyclagelosphaera lacuna*	*Bukrylithus ambiguus*	*Manivitella pemmatoidea*	*Axopodorhabdus cylindratus*	*Retecapsa octofenestrata*	*Retecapsa schizobrachiata*	*Nannoconus compressus*	*Tegumentum sp.*
3058-51		R	C											R		R				R	R							F	R	C	R
3058-45	R						R	A	F	R			R		R								R	F	R	R	R				
3058-35								C								R						R	R								
3058-25						R		C							F	R		R		R	R										
3031-19									R					R	C		R	R	R	R	R										
3031-12	R	R	R	C		R		R	R		R	R	R	R	R	R															
2925-33			F		C	C	C	C	R	R																					
2925-23-22		A	R	C																											
2925-14	R																														
3092-6																															
3092-1																															

Section 3	*Cyclagelosphaera margerelii*	*Nannoconus kamptneri subsp. minor*	*Watznaueria barnesiae*	*Watznaueria manivitiae*	*Nannoconus wintereri*	*Watznaueria communis*	*Zeugrhabdotus embergeri*	*Diazomatolithus lehmanii*	*Watznaueria britannica*	*Conusphaera mexicana*	*Nannoconus globulus subsp. minor*	*Nannoconus sp.*	*Cyclagelosphaera lacuna*	*Nannoconus steinmannii subsp. minor*	*Crepidolithus sp.*	*Zeugrhabdotus sp.*	*Helenea staurolithina*	*Nannoconus steinmannii subsp. steinmannii*
2921-13	C	C	C		C	C											R	
2921-7	F	C	C	C	C	C	R		C	R		R	R		R	R		F
2921-1																		
2920-1	C	A	C	C	A	C								F				
2920-10	C	C	A	A	R	A	R	R	C	R	R	F						

Section 2	*Helenea quadrata*	*Helenea staurolithina*	*Diazomatolithus lehmanii*	*Cretarhabdus madingleyensis*	*Parhabdolithus robustus*	*Cyclagelosphaera margerelii*	*Watznaueria barnesiae*	*Watznaueria fossacincta*	*Coccosphere*	*Watznaueria britannica*	*Watznaueria ovata*	*Zeugrhabdotus fissus*	*Zeugrhabdotus erectus*	*Ethmorhabdus gallicus*	*Watznaueria manivitiae*	*Cyclagelosphaera brezae*	*Zeugrhabdotus embergeri*	*Nannoconus wintereri*	*Nannoconus globulus subsp. minor*	*Watznaueria communis*	*Conusphaera mexicana*	*Nannoconus sp.*	*Nannoconus kamptneri subsp. minor*
2456-51						C	A	A									R	C	C	C	C		C
2456-41						C	A	F		F					F	F	F			C			
3056-31						C	A	A		C							R	C	C	C	C	C	
2456-23						A	A	F	F	F					C	C	F						
2456-12	C	C	R	R	R	VA	VA	C	R	C	R	R	R	R									
2456-1																							
2927-2																							

Section 1	*Cyclagelosphaera deflandrei*	*Zeugrhabdotus embergeri*	*Watznaueria fossacincta*	*Watznaueria britannica*	*Cyclagelosphaera margerelii*	*Watznaueria barnesiae*	*Watznaueria communis*	*Watznaueria manivitiae*	*Helenea chiastia*	*Manivitella pemmatoidea*	*Coccosphere*	*Cretarhabdus madingleyensis*	*Ethmorhabdus gallicus*	*Polycostella beckmannii*	*Conusphaera mexicana*	*Diazomatolithus lehmanii*	*Cyclagelosphaera lacuna*	*Zeugrhabdotus erectus*	*Nannoconus compressus*	*Polycostella senaria*	*Parhabdolithus robustus*	*Hexalithus noeliae*	*Cyclagelosphaera brezae*	*Helenea staurolithina*	*Hexalithus strictus*	*Cyclagelosphaera argoensis*
3112-3		R	C	C	A	A	R	C						C					R	R				R	R	R
3113-3		F	C	F	C	C	C	R					R		F	R		R		F		R	R			
2922-32C		C	C	C	C	C	C	R			R															
2923-13																										
2923-8		R	C	R	C	A	R							A	A											
2923-3																										
2901-94		F	C	C	C	C	R		E	R						R					R					
2901-87			C	R	C	C		R						R				R								
2901-82			A	F		A	R							C	C											
2901-77			A			A	R	R						A	A	R										
2901-72			A	F	C	A			F					C	R			F		F						
2901-65			C		C	C	R							C	R	R		R								
2901-61			C	F	C	C							R	C				R	R	R						
2901-59			C	R	C	C																				
2901-53	R	R	C	C	C	A								C	R	R	R	R								
2901-46	R		C	R	C	C			R																	
2901-36			C	F	F	C		F				R	R													
2901-19		R	C	R	C	C	R	R	R	R	R	R														
2901-5				R	R	F	R																			
2901-1	R	F	C	F	F	F																				

2011). However, this is significantly higher than the base of the *Calpionella alpina* Subzone, which is currently accepted as the marker of the Tithonian–Berriasian (Wimbledon 2017; Svobodová et al. 2019).

The FO of *Nannoconus steinmannii steinmannii* (sample 2921-7, Fig. 5G,H) is a major event that defines the base of NK-1 Zone in the Berriasian. Ammonites *Delphinella* cf. *tresannensis* and *Berriasella subcallisto* that characterize the *Grandis* Subzone were determined at this level of the section.

At the top of the Zavodskaya Balka section, at the level of sample 3058-25, the last occurrences of *Polycostella senaria, P. beckmanii,* and *Nannoconus wintereri* were fixed, which, together with the ammonite *Berriasella callisto*, has proved Berriasian age.

Discussion

It is remarkable that the FO of the subspecies *Nannoconus kamptneri minor* is assigned to beds characterized by ammonites of the *Grandis* Subzone (sample 2456-51) and corresponds to the top M18n magnetic Chron. It is about 80 m above the level of the Tithonian–Berriasian boundary determined on the basis of ammonites. According to Bakhmutov et al. (2018), *N. kamptneri minor* occurs approximately in the middle of the M19n.2n magnetic Subchron, and *N. steinmannii steinmannii* and *N. kamptneri kamptneri* — at the level of M18r magnetic Chron. If we consider the boundaries established by magnetostratigraphic data to be isochronous, then with respect to them, the boundaries established by nanofossils seem to be diachronous. This is confirmed by the analysis of numerous publications. Wimbledon et al. (2011) stated that the base of the NKT Zone is assigned to the top M19n magnetic Chron. In the Le Chouet section (France), the FADs of *Nannoconus steinmannii minor* and *N. kamptneri minor* correspond to the top M19n magnetic Chron (Wimbledon et al. 2013). A similar relationship has been observed in the section Barlya in the West Balkan Mts, Bulgaria (Lakova et al. 2017). In the Southern Alps, Casellato in Channell et al. (2010) determined the lower boundary of the Berriasian based on the FAD of *Nannoconus steinmannii minor* which is correlated with the M18r magnetic Chron. However, in the Torre de' Busi section, the base of the NKT Zone corresponds to the top M19n Chron, and in the Colme di Vignola section — to the top M18n Chron. In the Puerto Escaño section (Southern Spain), the boundary between the ammonite *Durangites* and *Jacobi* Zones has been assigned to the base of the M19n Chron, while the base of the NKT Zone has been traced at the top of the M19n Chron (Svobodová & Košťák 2016). In the Western Carpathians, the FAD of *N. steinmannii minor* has been fixed in the middle part of the M19n Chron (Michalík et al. 2016; Elbra et al. 2018) which is slightly above the Tithonian–Berriasian boundary level determined from calpionellids. In Hungary, in the Lókút section, the base of the NKT Zone has been determined at the top M19n2n Subchron (Grabowski et al. 2017). Thus, the position of the base of the NKT Zone varies from the top M19n Chron to the top M18n Chron. Therefore, the FAD of *Nannoconus steinmannii minor* could hardly be accepted as one of major markers of the Jurassic/Cretaceous boundary.

The integrated ammonite, calcareous nannofossil and magnetostratigraphic data obtained in studying the Feodosiyan sections may be applied to justify the boundary markers. The proximity of the base of the M18r Chron to the base of the *Grandis* Subzone in the Feodosiyan sections confirms the earlier declared opinion regarding the Tithonian–Berriasian boundary to be determined at the base of the ammonite *Grandis* Subzone (Arkadiev et al. 2018). In addition, the base of the NKT Zone is close to this level in the Feodosiyan section. The base of the *Calpionella alpina* Subzone in the Feodosiyan section is much lower (Platonov et al. 2014), but it is poorly defined due to the rarity of the finds and the poor preservation of the calpionellids.

Magnetostratigraphic interpretation

Petromagnetic and paleomagnetic data obtained independently from the both research teams are well-harmonized. The data on anisotropy of magnetic susceptibility and the results of the component analysis are equal in the papers of Bakhmutov et al. (2018) and Guzhikov et al. (2012). Also, the mean directions of characteristic remanent magnetization (ChRM) across the section obtained by different researchers statistically coincide. The paleomagnetic column of the outcrop at the boathouse [outcrop B in Bakhmutov et al. (2018) and outcrops 2920, 2921 in Arkadiev et al. (2018); Guzhikov et al. (2012)] is similar. The reverse polarity magnetic zone (R) at the top of the composite section has been interpreted as the M17r Chron by all authors (Fig. 7).

However, the paleomagnetic column and results of magnetopolar interpretations of the Cape Saint Ilya section vary and have been done by different researchers, as in the cases of outcrops A and 1–6 (Bakhmutov et al. 2018) and outcrop 2456 (Arkadiev et al. 2018; Guzhikov et al. 2012).

In our opinion, the outcrop A in Bakhmutov et al. (2018), namely the Feodosiyan Marls under the light tower, duplicates the outcrop B. We came to such a conclusion after we had restudied in detail the section structure in 2016. If our approach to comparison of the outcrops is meaningful, then the R-Zone [top part of the outcrop 4 in Bakhmutov et al. (2018)], which is the next reversal zone down-section, should rather be the M18r Chron, than the M19n.1r Subchron ("Brodno") (Fig. 7). The analysis of magnetostratigraphic data along the entire composite Upper Tithonian–Lower Berriasian section (Arkadiev et al. 2018; Guzhikov et al. 2012) confirms that this R-Zone cannot be the analogue of the M19n.1r Subchron. Admitting the contrary, it should be concluded that two underlying R-Zones assigned to beds hosting *Neoperisphinctes* cf. *falloti* and *Paraulacosphinctes* cf. *transitorius* should be interpreted as the M19r and M20r Chrons, respectively. However, such an interpretation is not applicable from the view point of the ammonite stratigraphy since predominantly the Early

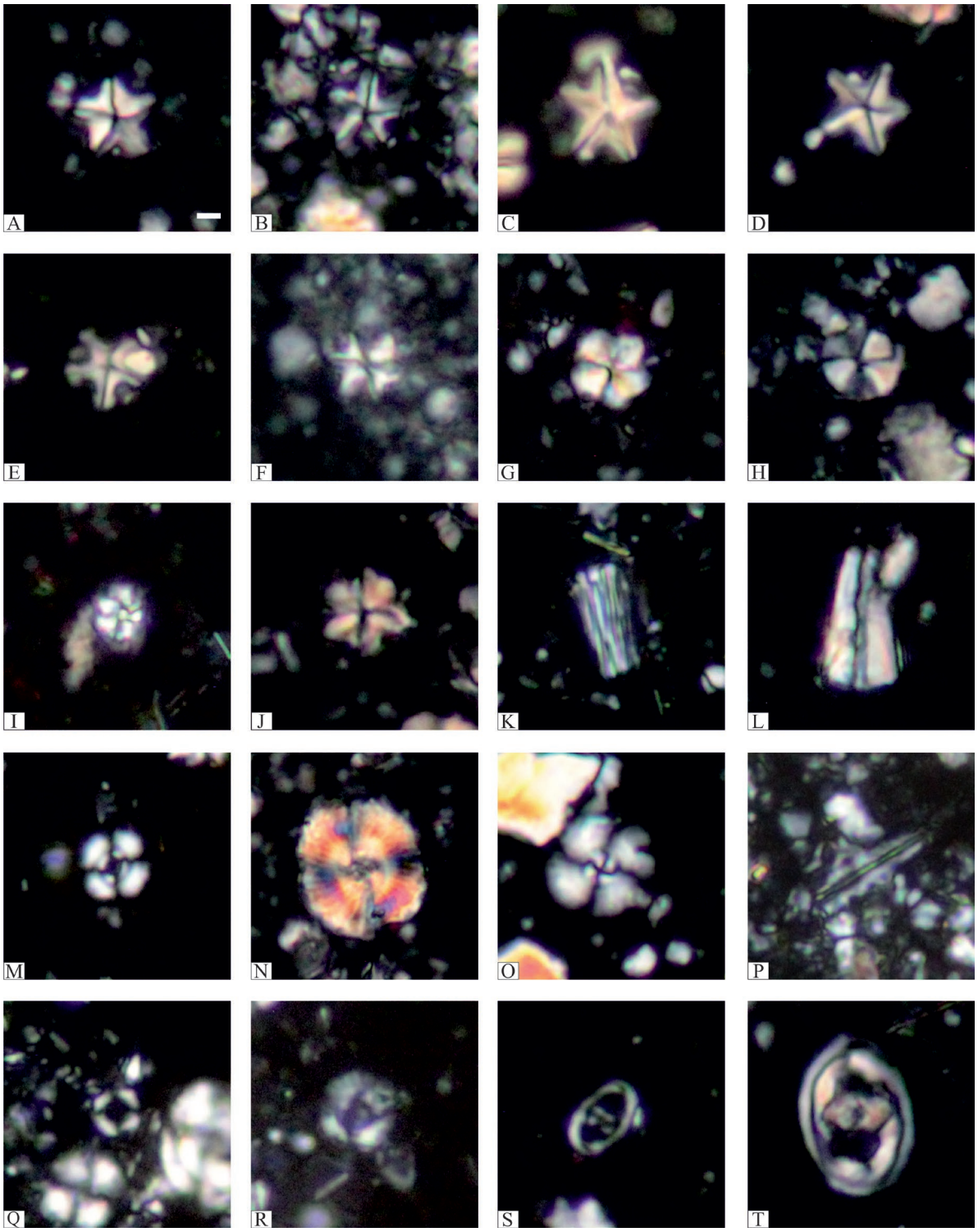

Fig. 3. Calcareous nannofossils from the Feodosiyan section. All photomicrographs under polarized light; scale bar=2 μm. **A** — *Micrantholithus obtusus* Stradner (sample 2925-33); **B–D** — *Micrantholithus parvistellatus* Varol (sample 2925-14); **E** — *Micrantholithus* sp (sample 2925-14); **F** — *Hexalithus strictus* Bergen (sample 3112-3). **G–H** — *Hexalithus noeliae* Loeblich & Tappan (sample 3113-3); **I** — *Polycostella beckmannii* Thierstein (sample 2901-53); **J** — *Polycostella senaria* Thierstein (sample 3092-6); **K–L** — *Conusphaera mexicana* Trejo (sample 3058-51); **M** — *Cyclagelosphaera lacuna* Varol & Girgis (sample 2901-53); **N** — *Cyclagelosphaera deflandrei* (Manivit) Roth (sample 2901-1); **O** — *Cyclagelosphaera margerelii* Noël (sample 2921-7); **P** — *Lithraphidites carniolensis* Deflandre (sample 2925-14); **Q** — *Diazomatolithus galicianus* de Kaenel & Bergen (sample 3031-19); **R** — *Diazomatolithus lehmanii* Noël (sample 3031-12); **S** — *Zeugrhabdotus diplogrammus* (Deflandre in Deflandre & Fert) Burnett in Gale et al (sample 3031-12); **T** — *Zeugrhabdotus embergeri* (Noël) Perch-Nielsen (sample 3058-51).

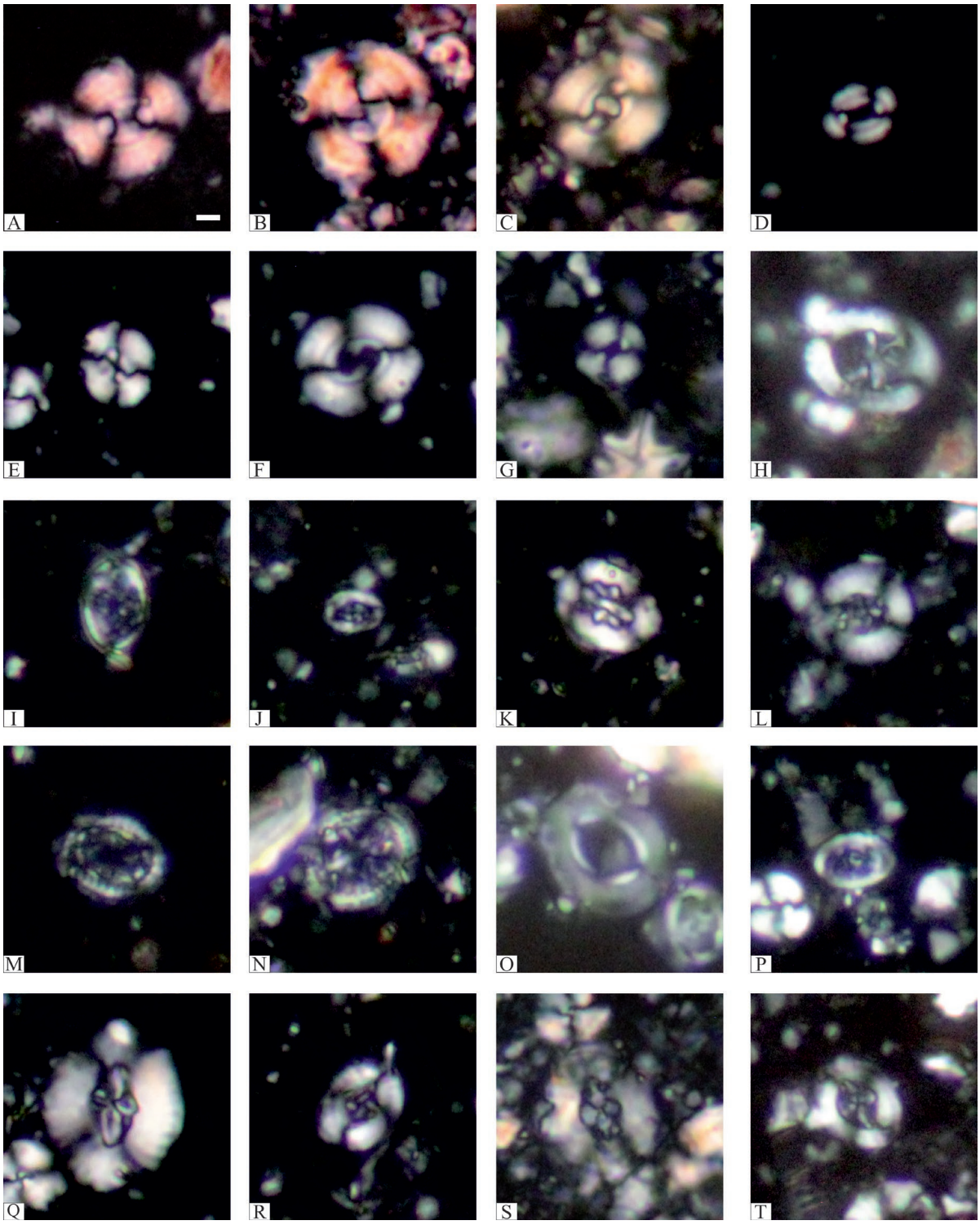

Fig. 4. Calcareous nannofossils from the Feodosiyan section. All photomicrographs under polarized light; scale bar=2 μm. **A** — *Watznaueria communis* Reinhardt (sample 3113-3); **B** — *Watznaueria manivitiae* Bukry (sample 2901-36); **C** — *Watznaueria britannica* (Stradner) Reinhardt (sample 2456-12); **D** — *Watznaueria ovata* Bukry (sample 2456-12); **E** — *Watznaueria barnesiae* (Black in Black & Barnes) Perch-Nielsen (sample 3112-3); **F** — *Watznaueria biporta* Bukry (sample 3031-12); **G** — *Watznaueria fossacincta* (Black) Bown in Bown & Cooper (sample 2901-19); **H** — *Speetonia colligata* Black (sample 3058-35); **I** — *Percivalia fenestrata* (Worsley) Wise (sample 3092-6); **J** — *Eiffellithus primus* Applegate & Bergen (sample 3058-25); **K** — *Retecapsa angustiforata* Black (sample 2925-14); **L** — *Retecapsa surirella* (Deflandre & Fert) Grün in Grün and Allemann (sample 3058-45); **M** — *Ethmorhabdus gallicus* Noël (sample 2901-61); **N** — *Axopodorhabdus cylindratus* (Noël) Wind and Wise in Wise and Wind (sample 2901-36); **O** — *Tubodiscus verenae* Thierstein (sample 3031-19); **P** — *Rhagodiscus asper* (Stradner) Reinhardt (sample 3058-45); **Q** — *Cruciellipsis cuvillieri* (Manivit) Thierstein (sample 3058-45); **R** — *Helenea quadrata* (Worsley) Rutledge & Bown in Bown et al. (sample 3058-51); **S** — *Helenea chiastia* Worsley (sample 2901-19); **T** — *Helenea staurolithina* Worsley (sample 3031-12).

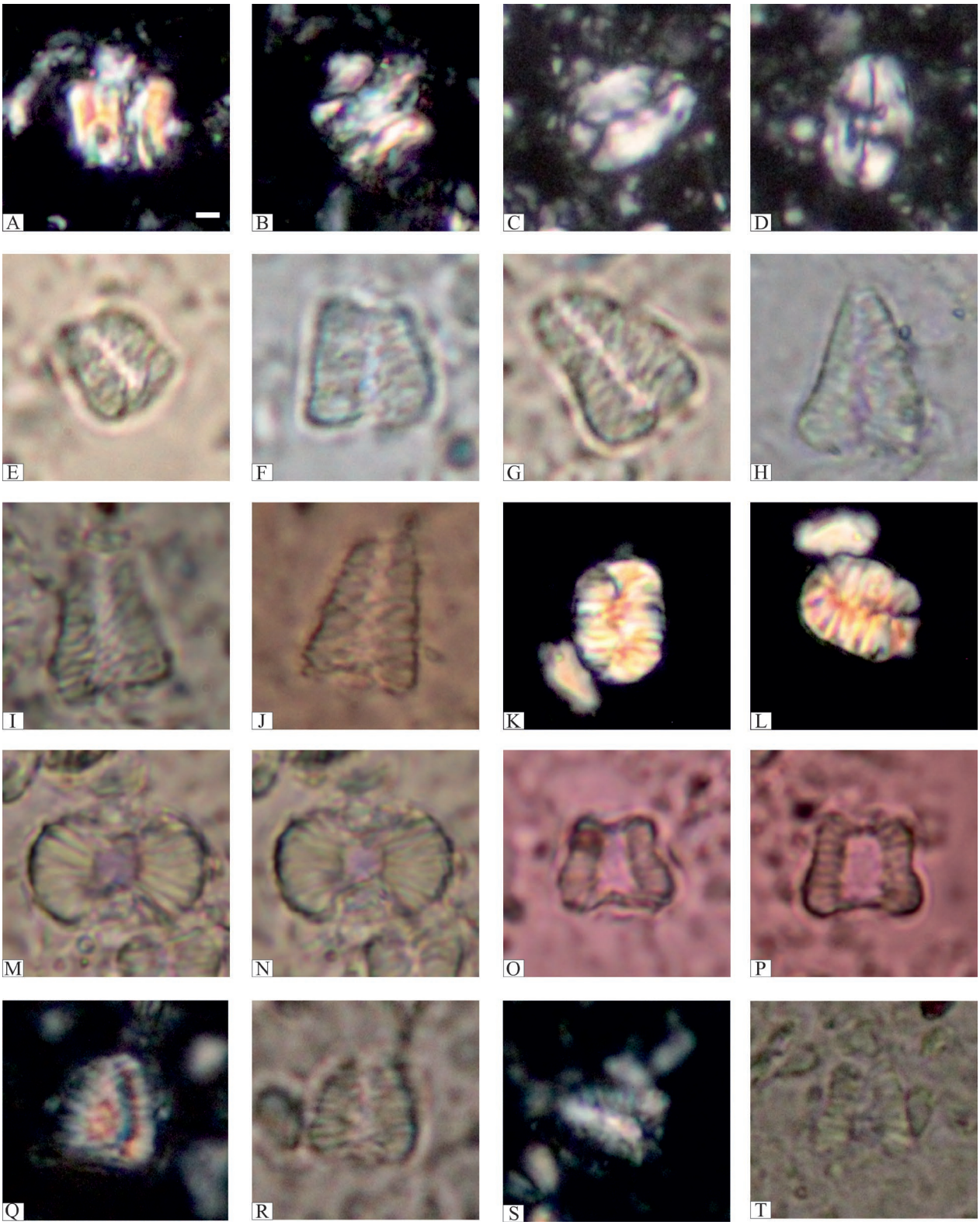

Fig. 5. Calcareous nannofossils from the Feodosiyan section. All photomicrographs under polarized light; scale bar=2 μm. **A, B** — *Parhabdolithus robustus* Noël (sample 2901-94); **C, D** — *Crepidolithus* sp. (sample 2921-7); **E, F** — *Nannoconus steinmannii* subsp. *minor* (Kamptner) Deres and Achéritéguy (sample 2920-1); **G, H** — *Nannoconus steinmannii* subsp. *steinmannii* Kamptner (sample 2921-7); **I, J** — *Nannoconus kamptneri* subsp. *kamptneri* Brönnimann (sample 3092-6); **K, L** — *Nannoconus compressus* Bralower & Thierstein in Bralower et al. (sample 2901-61); **M, N** — *Nannoconus globulus* subsp. *minor* (Brönnimann) Bralower in Bralower et al. (sample 2925-33); **O, P** —*Nannoconus wintereri* Bralower & Thierstein, in Bralower et al. (sample 2456-31); **Q–T** — *Nannoconus kamptneri* subsp. *minor* Bralower (sample 2456-51).

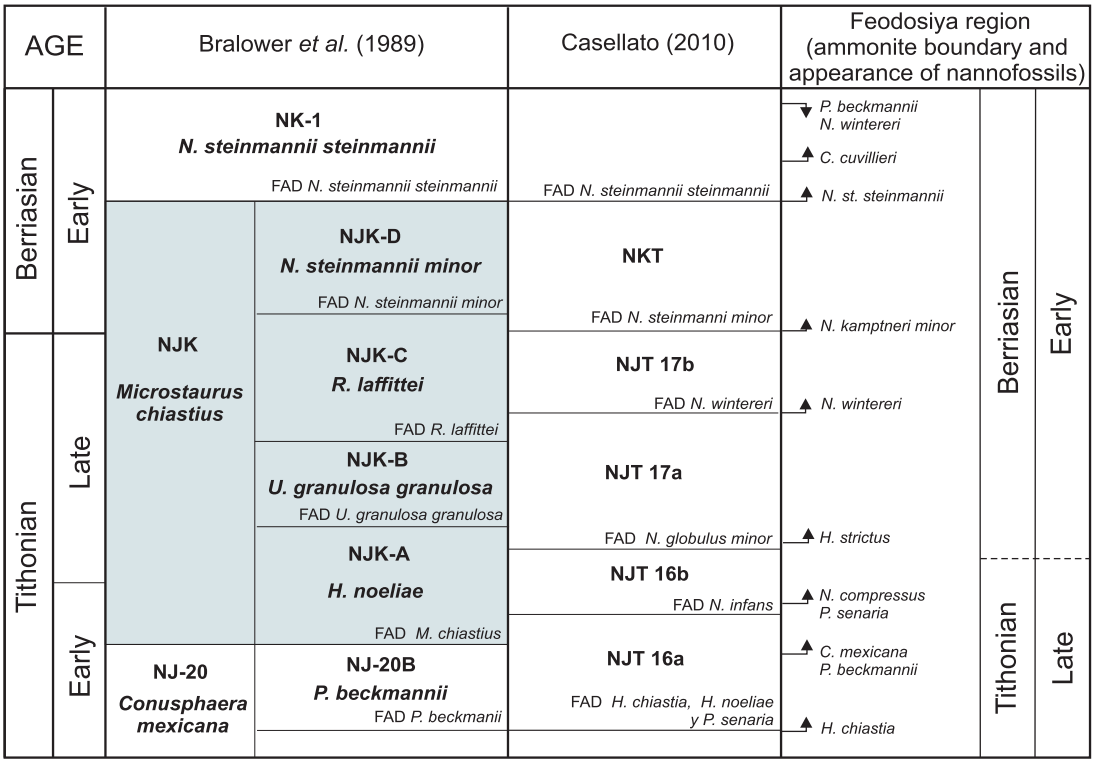

Fig. 6. Calcareous nannofossil zonation of the Tithonian–Berriasian interval and main bio-events according to Bralower et al. (1989), Casellato (2010). Ammonite boundary of Tithonian–Berriasian and appearance of nannofossils in Feodosiya region.

Tithonian age of the M20r Chron is substantiated in the key sections of different regions (Grabowski et al. 2010; Houša et al. 1999; Lukeneder et al. 2010; Pruner et al. 2010), while the oldest sediments we have studied in the Feodosiyan sections have been assigned to the Upper Tithonian on the basis of ammonite finds (Arkadiev et al. 2018; Guzhikov et al. 2012).

The paleomagnetic section and petromagnetic diagrams (magnetic susceptibility) corresponding to the top of the outcrop 2456 (Guzhikov et al. 2012) are well correlated with the data of the outcrops 5 and 6 and top of the outcrop 4 (Bakhmutov et al. 2018) (Fig. 7). It is obvious that different authors studied the same interval of the section.

The lower part of the outcrop 2456 (Guzhikov et al. 2012) and the outcrop 1 (Bakhmutov et al. 2018) are undoubtedly the same research subject because their bases represent a lithological benchmark — a 3 m-thick bed of conglomerate-type limestone (the base of the package 10 according to Guzhikov et al. (2012) that crops out in the area of Cape Saint Ilia approximately at sea level. Both groups of researchers registered there an alternated polarity as alternation of four intervals of anomalous polarity (Guzhikov et al. 2012; Arkadiev et al. 2018) (Fig. 7). According to the data of Bakhmutov and his colleagues, a large number of bipolar intervals are obviously associated with a higher density of sampling in this part of the section: they sampled about 20 levels while we did only 7. The earlier assumption was that the zone of bipolar polarity is assigned to the bottom of the M18r Chron (Guzhikov et al. 2012; Arkadiev et al. 2018) but, perhaps, it is more reasonable not to identify this magnetic zone with magnetic chrons in view of its anomalous character as was done by Bakhmutov et al. (2018).

Close to the boundary between the packages 10 and 11 (Arkadiev et al. 2018), a gap in sampling, which we did not cover in our work, can really be available (Guzhikov et al. 2012). Up to now, we have not managed to assess the thickness of the gap, but we assume that it is not large. Moreover, we could not find the sediments near the Cape Saint Ilya [including areas where the outcrops 2 and 3 are situated, according to Bakhmutov et al. (2018)], which could be securely defined as those corresponding to the gap. In our opinion, the thickness of this gap mentioned by Bakhmutov et al. (2018) is significantly exaggerated, and the outcrops 2 and 3 may have the same beds multiplied more than once. We believe that whatever the case, this matter should be additionally studied.

On the basis of the currently existing data, it is not inconceivable that the interval covering outcrop 4, which does not have determinations of the magnetic polarity (Bakhmutov et al. 2018), corresponds to an extension of a reversed polarity zone. In all cases, it is premature to interpret the bottom part of outcrop 4 as an interval of normal (N) polarity (Bakhmutov et al. 2018).

New data on calcareous nannofossils herein presented have confirmed the eligibility of the explanation we outlined for contradictions between results of the magnetostratigraphic interpretation of our data, on one side, and those of Bakhmutov et al. (2018), on the other (Fig. 7).

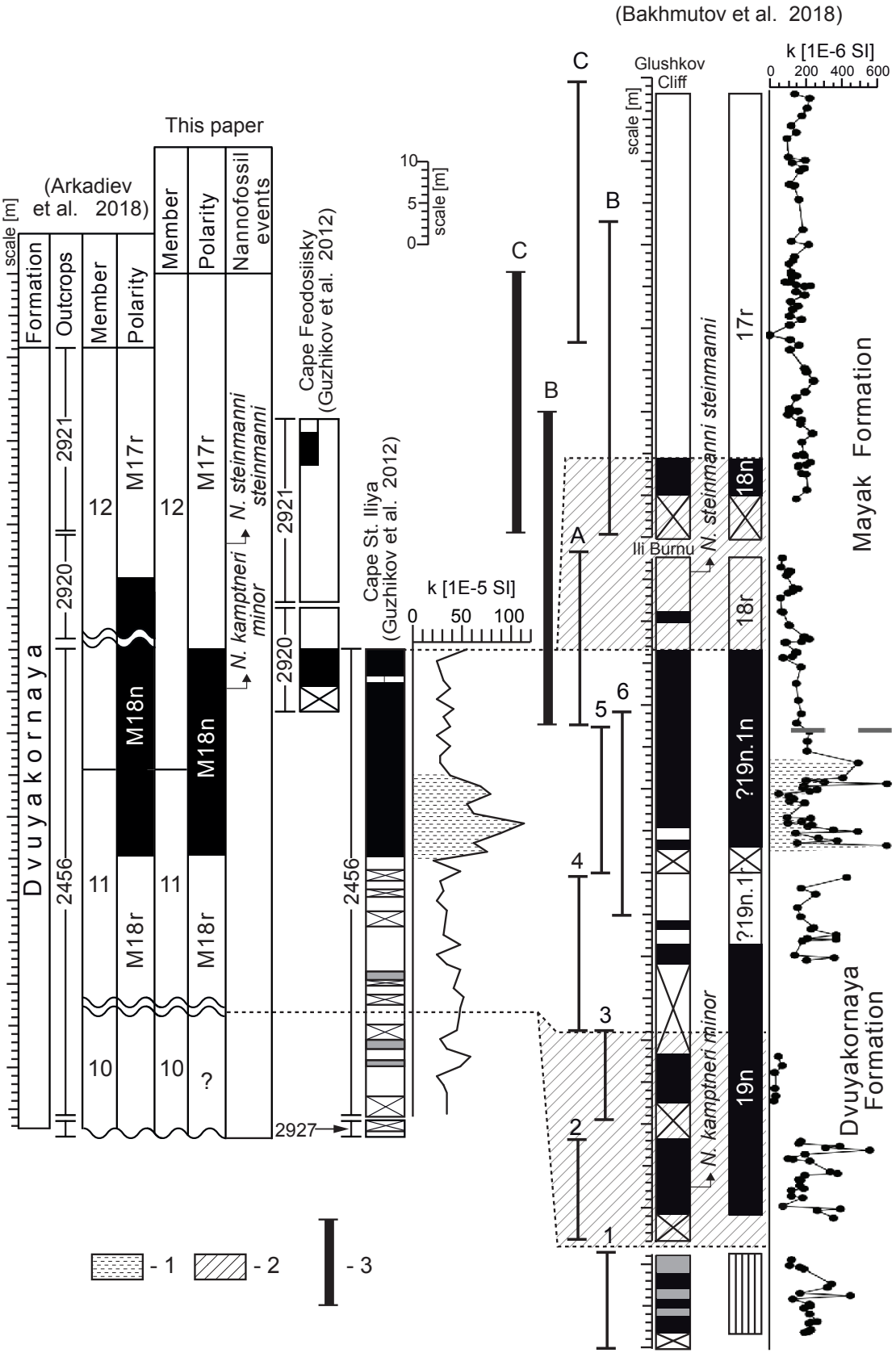

Fig. 7. Correlation of compiled magnetostratigraphic sections of Feodosiyan Lower Berriasian produced on the basis of our data (Guzhikov et al. 2012; Arkadiev et al. 2018) and data of Bakhumtov et al. (2018). 1 — interval with increased magnetic susceptibility; 2 — intervals mistakenly included in the composite section (Bakhmutov et al. 2018); 3 — true positions of outcrops B and C relative to outcrop A.

The FAD of *N. kamptneri minor* has been assigned by Bakhmutov et al. (2018) to the middle of the outcrop 2, which testifies in favour of our version about duplicating of the same intervals of the section. Presumably, the outcrops 2 and 3 duplicate the outcrops 5 and 6, while we (in the outcrop 2456) and Bakhmutov et al. (2018) fixed approximately the same level of the FAD of *N. kamptneri minor* (Fig. 7).

According to the interpretation of Bakhmutov et al. (2018), the FADs of *N. steinmannii steinmannii* and *N. kamptneri kamptneri* were assigned to the M18r Chron. It contradicts to the data given by the same authors on the age dispersion of nannofossils associations (fig. 24 in Bakhmutov et al. 2018), according to which the FADs of these subspecies are assigned to base of the M17r Chron. This contradiction is cleaned away in our version, according to which the top of the Cape Saint Ilya section (outcrop A) duplicates the section near the boat-house (base of the outcrop B) (Fig. 7).

If one admits the rightness of our version, the FADs of nannofossil taxa in the section on the data of Bakhmutov et al. (2018) is much better correlated with the new data about the age dispersion of FADs of nannofossils associations (fig. 24 in the paper of Bakhmutov et al. 2018) (Fig. 8).

The interval between the uppermost findings of Upper Tithonian ammonites and the lowest findings of Lower Berriasian ammonites is over 100 metres in the Dvuyakornaya Bay section, which extends downwards the Cape Saint Ilya section (Arkadiev et al. 2018). The target to justify more accurately the level of the base of Jacobi Zone in the Feodosiyan section like in other sections of the Mountainous Crimea is quite challenging. The level of the Grandis Subzone base, which is close to the base of the NKT nannofossil Zone has been determined and traced much better. Unfortunately, we have not managed to distinguish the base of the magnetic M18r Chron. Most likely, this level is located in the sampling gap between the Dvuyakornaya Bay and Cape Saint Ilya sections (refer to fig. 20 in Arkadiev et al. 2018). It is not improbable that the zone of mixed (unknown) polarity at the bottom of the Cape Saint Ilya section, which is allocated both by Guzhikov et al. (2012) and Bakhmutov et al. (2018) (Fig. 7), corresponds to the geomagnetic reversal epoch between the M19 and M18 Chrons. Whatever the case, the lowest boundary of M18r is situated in the Feodosiyan section below the base of the *Grandis* Subzone and above the *Jacobi* Subzone bottom. If our assumptions regarding the small thickness of gaps in the composite section are correct, then the M18r bottom in the section is likely close to the base of the *Grandis* Subzone**.**

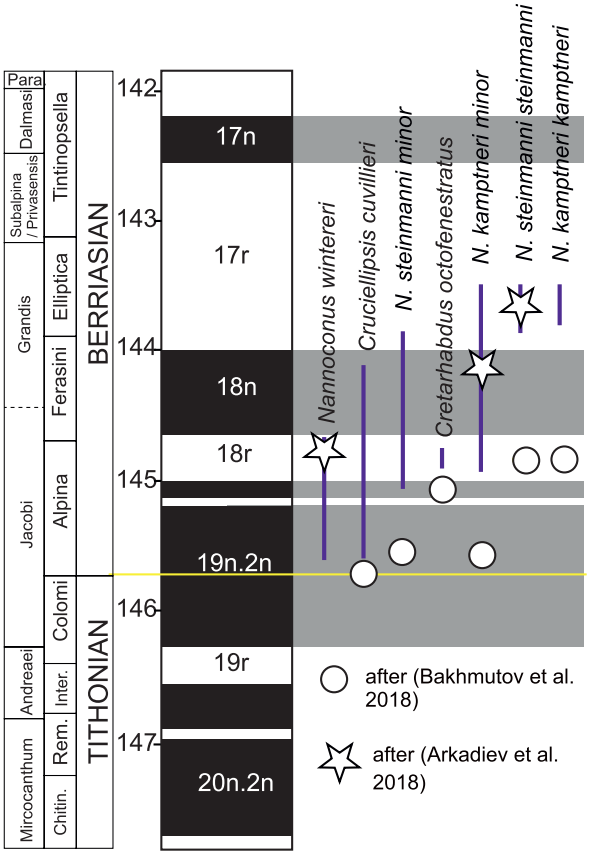

Fig. 8. Correlation of first occurrences of calcareous nannofossils (FO) in the Lower Berriasian Feodosiyan section (this paper) with data of Bakhmutov et al. and FAD range in different regions (refers to fig. 24, Bakhmutov et al. 2018).

Lithostratigraphic notes

In the top part of the Dvuyakornaya Formation (the package of Feodosiyan Marls), Bakhmutov et al. (2018) has introduced as a new formation, the so-called Mayak Formation. At first this name was proposed in abstracts of the meeting of the Berriasian Working Group held in Slovakia (Bakhmutov et al. 2016). "Dvuyakornaya Formation" is a widely used and well-established name in literature. Initially, the formation was distinguished by Astakhova et al. (1984). The detailed lithological and paleontological description of the formation has been provided in our publications (Arkadiev et al. 2012, 2018). In Bakhmutov et al. (2016), it is mentioned that the Feodosiyan Marls occur above the Dvuyakornaya Formation. However, Astakhova et al. (1984, p. 62) considered the Feodosiyan Marls as the facial analogue of the clays and limestones of the Dvuyakornaya and base of the Sultanovskaya formations. In our opinion, changing the name and volume of the existing formation is not reasonable. It will just lead to some additional complications in the matter of formation stratification of the Upper Jurassic–Lower Cretaceous interval of Mountainous Crimea.

Conclusion

New data about calcareous nannofossils from the Feodosiyan section significantly enlarges its characteristics and highlights this section as one of the best in terms of degree of description of details of the Jurassic–Cretaceous boundary interval for the Tethys. The base of the NKT Zone and likely

the lower boundary of the M18r magnetic chron are close to the base of the ammonite *Grandis* Subone, which allows highlighting of the base of the *Grandis* Subzone as the Tithonian/Berriasian (Jurassic/Cretaceous) boundary rather than the base of the *Jacobi* Zone/Subzone.

Acknowledgements: The authors thank Valentina Koval for help in translating the paper into English. We are very grateful to K. Stoykova and I. Lakova (Geological Institute, Bulgarian Academy of Sciences) for linguistic proofreading and very constructive comments, which greatly improved the text of the manuscript.

References

Arkadiev V.V., Bogdanova T.N., Guzhikov A.Yu., Lobacheva S.V., Myshkina N.V., Platonov E.S., Savelyeva Yu.N., Shurekova O.V. & Yanin B.T. 2012: Berriasian stage of the Mountainous Crimea. *LEMA Publishing House,* Saint Petersburg, 1–472 (in Russian).

Arkadiev V.V., Guzhikov A.Yu, Savelieva Yu.N., Feodorova A.A., Shurekova O.V., Bagaeva M.I., Grishchenko V.A. & Manikin A.G. 2015: New Data on Bio- and Magnetostratigraphy of the Upper Berriasian Zavodskaya Balka section (Eastern Crimea, Feodosiya). *Bull. Saint Petersburg St. Univ., Geology* 7, 4, 4–36 (in Russian).

Arkadiev V.V., Grishchenko V.A., Guzhikov A.Yu., Manikin A.G., Savelieva Yu.N., Feodorova A.A. & Shurekova O.V. 2017: Ammonites and Magnetostratigraphy of the Berriasian–Valanginian Boundary Deposits from Eastern Crimea. *Geol. Carpath.* 68, 6, 505–516.

Arkadiev V., Guzhikov A., Baraboshkin E., Savelieva Ju., Feodorova A., Shurekova O., Platonov E. & Manikin A. 2018: Biostratigraphy and Magnetostratigraphy of the Upper Tithonian–Berriasian of the Crimean Mountains. *Cretaceous Res.* 87, 5–41.

Astakhova T.V., Gorak S.V., Kraeva E.Y., Kulichenko V.G., Permyakov V.V., Plotnikova L.F., Semenenko V.N., Barchenko O.I., Blagodarov M.I., Bugaets A.T., Bondarenko V.G., Borisenko L.S., Vanina M.V., Vdovenko M.V., Voronov M.A., Gorbach L.P., Grigoriev A.V., Gurevich K.Y., Dulub V.G., Isagulova E.Z., Korbut Y.B., Kotlyar O.E., Konenkova D.I., Makarenko D.E., Menkes M.A., Nerodenko V.M., Novik N.N., Naga V.I., Plakhotnogo L.G., Pyatkova D.M., Romanov L.F., Savron E.B. Slyusar B.S., Sulimov I.N., Teslenko Y.V., Fedorov P.V., Tsegelnyk P.D. & Yanovskaya G.G. 1984: Geology of Shelf of the UkrSSR. Stratigraphy (Shelf and Black Sea Coast). *Naukova Dumka,* Kiev, 1–184 (in Russian).

Bakhmutov V.G., Casellato C.E., Halásová E., Ivanova D.K., Reháková D. & Wimbledon W.A.P. 2016: Bio- and Magnetostratigraphy of the Upper Tithonian–Lower Berriasian in Southern Ukraine. XIIth Jurassica Conference. In: Michalík J. & Fekete K. (Eds.): Workshop of the ICS Berriasian Group and IGCP 632. Field Trip Guide and Abstracts Book. *Earth Science Institute, Slovak Academy of Sciences,* Bratislava, 97–100.

Bakhmutov V.G., Halásová E., Ivanova D.K., Józsa S., Reháková D. & Wimbledon W.A.P. 2018: Biostratigraphy and magnetostratigraphy of the uppermost Tithonian–Lower Berriasian in the Theodosia area of Crimea (Southern Ukraine). *Geol. Quarterly* 62, 2, 197–236.

Baraboshkin E.Yu., Arkadiev V.V. & Kopayevich L.F. 2016a: Reference sections of the Cretaceous System of the Mountainous Crimea. Guidebook of the Field Excursions of the 8th All-Russian meeting, September 26–October 3, 2016. *ChernomorPress Publishing House,* Simferopol, 1–90 (in Russian).

Baraboshkin E.Yu., Baraboshkin E.E., Yanin B.T. & Piskunov V.K. 2016b: Tithonian–Berriasian deep-water ichnoassemblages of Feodosiya (Republic of Crimea). In: E.Yu. Baraboshkin (Ed.): The Cretaceous System of Russia and Neighbouring Countries: Problems of Stratigraphy and Paleogeography. Materials of the VII All-Russian Conference, September 26–October 3, 2016, Republic of Crimea. *Chernomorpress Publishing House,* Simferopol, 45–48 (in Russian).

Baraboshkin E.Yu., Guzhikov A., Arkadiev V. & Baraboshkin E.E. 2017: New Data on the Berriasian Stage of the Crimea. In: 10th International Symposium on the Cretaceous. Vienna, August 21–26, 2017. Abstracts. *Berichte der Geol. Bundesanst.* 120, 23.

Baraboshkin E.Yu., Arkadiev V.V., Guzhikov A.Yu. & Baraboshkin E.E. 2019: Tirnovella occitanica Zone of the Berriassian in Feodosiya region (Eastern Crimea). *Moscow University Geology Bull.* 1, 25–35 (in Russian).

Bralower T.J., Monechi S. & Thierstein H.R. 1989: Calcareous Nannofossil Zonation of the Jurassic–Cretaceous Boundary Interval and Correlation with the Geomagnetic Polarity Timescale. *Mar. Micropaleont.* 14, 153–235.

Casellato C.E. 2010: Calcareous Nannofossil Biostratigraphy of Upper Callovian–Lower Berriasian from the Southern Alps, North Italy. *Rivista Italiana di Paleontologia e Stratigrafia* 116, 357–404.

Channell J.E.T., Casellato C.E., Muttoni G. & Erba E. 2010: Magnetostratigraphy, Nannofossil Stratigraphy and Apparent Polar Wander for Adria–Africa in the Jurassic–Cretaceous Boundary Interval. *Palaeogeogr. Palaeoclimatol. Palaeoecol.* 293, 51–75.

Dorotyak Yu.B., Matveyev A.V. & Schevchuk Ye.A. 2009: Micropaleontologic characteristic of the boundary Jurassic–Cretaceous deposits of the Mountain Crimea by foraminifers, calcareous nannoplankton, dinocysts, spores, and pollen. In: Fossil flora and fauna of Ukraine: paleoecological and stratigraphic aspects. *Proceedings of the Institute of Geological Sciences of the National Academy of Sciences of Ukraine*, Kiev, 108–117 (in Ukrainian with an English abstract).

Edwards A. 1963: A preparation technique for calcareous nannoplankton. *Micropaleontology* 9, 103–104.

Elbra T., Bubík M., Reháková D., Schnabl P., Čížková K., Pruner P., Kdýr Š., Svobodová A. & Švábenická L. 2018: Magneto- and biostratigraphy across the Jurassic–Cretaceous Boundary in the Kurovice section, Western Carpathians, Czech Republic. *Cretaceous Res.* 89, 211–223.

Grabowski J., Haas J., Márton E. & Pszczółkowski A. 2010: Magneto- and biostratigraphy of the Jurassic/Cretaceous boundary in the Lókút section (Transdanubian range, Hungary). *Stud. Geophys. Geod.* 54, 1–26.

Grabowski J., Haas J., Stoykova K., Wierzbowski H., Brański P. 2017: Environmental Changes around the Jurassic/Cretaceous Transition: New Nannofossil, Chemostratigraphic and Stable Isotope Data from the Lókút Section (Transdanubian Range, Hungary). *Sediment. Geol.* 360, 54–72.

Guzhikov A.Yu., Arkad'ev V.V., Baraboshkin E.Yu., Bagaeva M.I., Piskunov V.K., Rud'ko S.V., Perminov V.A. & Manikin A.G. 2012: New sedimentological, bio-, and magnetostratigraphic data on the Jurassic–Cretaceous boundary interval of Eastern Crimea (Feodosiya). *Stratigraphy and Geological Correlation* 20, 3, 261–294.

Houša V., Krs M., Krsová M., Man O., Pruner P. & Venhodová D. 1999: High-resolution magnetostratigraphy and micropaleontology across the J/K boundary strata at Brodno near Žilina, western Slovakia: summary results. *Cretaceous Res.* 20, 699–717.

Lakova I., Grabowski J., Stoykova K., Petrova S., Reháková D., Sobień K. & Schnabl P. 2017: Direct correlation of Tithonian/Berriasian boundary calpionellid and calcareous nannofossil events in the frame of magnetostratigraphy: new results from the West Balkan Mts, Bulgaria, and review of existing data. *Geol. Balcanica* 46, 2, 47–56.

Lukeneder A., Halásová E., Kroh A., Mayrhofer S., Pruner P., Reháková D., Schnabl P., Sprovieri M. & Wagreich M. 2010: High resolution stratigraphy of the Jurassic–Cretaceous boundary interval in the Gresten Klippenbelt (Austria). *Geol. Carpath.* 61, 4, 365–381.

Matveyev A.V. 2009: Tithonian Calcareous Nannoplankton of the Eastern Crimea. In: Fossil flora and fauna of Ukraine: paleoecological and stratigraphic aspects. *Proceedings of the Institute of Geological Sciences of the National Academy of Sciences of Ukraine*, Kiev, 104–107 (in Ukrainian with an English abstract).

Matveyev A.V. 2010: Lower Berriasian Calcareous Nannoplankton of Mountainous Crimea. In: Cretaceous System of Russian and FSU. Materials of the V All-Russian Meeting. 23–28 August 2010, Ulyanovsk. *Ulyanovsk State University Press,* 251–256 (in Russian).

Michalík J. & Reháková D. 2011: Possible Markers of the Jurassic/Cretaceous Boundary in the Mediterranean Tethys: a Review and a State of Art. *Geoscience Frontiers* 2, 475–490.

Michalík J., Reháková D., Grabowski J., Lintnerová O., Svobodová A., Schlögl J., Sobień K. & Schnabl P. 2016: Stratigraphy, plankton communites, and magnetic proxies at the Jurassic/Cretaceous boundary in the Pieniny Klippen Belt (Western Carpathians, Slovakia). *Geol. Carpath.* 67, 4, 303–328.

Platonov E., Lakova I., Petrova S. & Arkadiev V. 2014: Tithonian and Lower Berriasian calpionellid against ammonite biostratigraphy of the Dvuyakornaya Formation in eastern Crimea. *Geol. Balcanica* 43, 1–3, 63–76.

Pruner P., Houša V., Olóriz F., Košťák M., Krs M., Man O., Schnabl P., Venhodová D., Tavera J.M. & Mazuch M. 2010: High-resolution magnetostratigraphy and biostratigraphic zonation of the Jurassic/Cretaceous boundary strata in the Puerto Escaño section (Southern Spain). *Cretaceous Res.* 31, 192–206.

Retowski O. 1893: Die tithonischen Ablagerungen von Theodosia. *Bull. Soc. Natur. Mosc. N. sér.* 7, 2–3, 206–301.

Savelieva Yu.N., Shurekova O.V., Feodorova A.A., Arkadiev V.V., Grishchenko V.A., Guzhikov A.Yu. & Manikin A.G. 2017: Microbiostratigraphy of the Berriasian–Valanginian boundary in Eastern Crimea: foraminifers, ostracods, organic-walled dinoflagellate cysts. *Geol. Carpath.* 68, 6, 517–529.

Sokolov V.D. 1886: Materials on Geology of Crimea. Crimea Tithonian. *Bull. of Moscow Soc. Devotees Nat. Sci., Anthropology and Ethnography* XIV, 1–43 (in Russian).

Stoykova K., Idakieva V., Ivanov M. & Reháková D. 2018a: Calcareous nannofossil and ammonite integrated biostratigraphy across the Jurassic–Cretaceous boundary strata of the Kopanitsa composite section (West Srednogorie Unit, Southwest Bulgaria). *Geol. Carpath*. 69, 2, 199-217.

Stoykova K., Michalík J., Petrova S., Reháková D., Idakieva V., Ivanov M. & Andreeva P. 2018b: Correlation of the Jurassic/Cretaceous boundary sequences in the sections of West Srednogorie, Bulgaria, based on micro- and macrofossil data and sea level changes. *Review of the Bulgarian Geological Society* 79, 3, 103–104.

Svobodová A. & Košťák M. 2016: Calcareous nannofossils of the Jurassic/Cretaceous boundary strata in the Puerto Escaño Section (Southern Spain) — biostratigraphy and paleoecology. *Geol. Carpath.* 67, 3, 223–238.

Svobodová A., Švábenická L., Reháková D., Svobodová M., Skupien P., Elbra T. & Schnabl P. 2019: The Jurassic/Cretaceous boundary and high resolution biostratigraphy of the pelagic sequences of the Kurovice section (Outer Western Carpathians, the northern Tethyan margin). *Geol. Carpath.* 70, 2, 153–182.

Wimbledon W.A.P. 2017: Developments with fixing a Tithonian/Berriasian (J/K) boundary. *Volumina Jurassica* XV, 181–186.

Wimbledon W.A.P., Casellato C.E., Reháková D., Bulot L.C., Erba E., Gardin S., Verreussel R.M., Munsterman D.K. & Hunt C.O. 2011: Fixing a Basal Berriasian and Jurassic–Cretaceous (J–K) Boundary — is there perhaps some light at the end of the tunnel? *Rivista Italiana di Paleontologia e Stratigrafia* 117, 295–307.

Wimbledon W.A.P., Reháková D., Pszczółkowski A., Casellato C.E., Halásová E., Frau C., Bulot L.G., Grabowski J., Sobień K., Pruner P., Schnabl P. & Čížková K. 2013: An Account of the Bio- and Magnetostratigraphy of the Upper Tithonian–Lower Berriasian Interval at Le Chouet, Drôme (SE France). *Geol. Carpath.* 64, 6, 437–460.